WIND TURBULENCE INPUTS FOR HORIZONTAL AXIS WIND TURBINES

W.E. Holley, R.W. Thresher, and S-R. Lin

Department of Mechanical Engineering
Oregon State University
Corvallis, OR 97331

1. INTRODUCTION

In order to predict wind turbine response characteristics in the presence of atmospheric turbulence, two major modeling steps are required. First, the important atmospheric sources for the force excitations felt by the wind turbine system must be identified and characterized. Second, a dynamic model must be developed which describes how these excitations are transmitted through the structure and power train. The goal of this paper is to establish the first modeling step, that of quantifying the important excitations due to the atmospheric turbulence. The dynamic modeling of the second step is undertaken in the accompanying paper (1).

Fluctuations in the aerodynamic forces on a wind turbine blade are generated by the relative motions of the air with respect to the blade. These relative motions are comprised of two parts: the motions of the blade and the motions of the air. The motions of the air can further be divided into the undisturbed turbulent flow and the "induced flow" due to the presence of the wind turbine wake. The terms comprising the undisturbed flow will be characterized in this paper. More precisely, for a horizontal axis wind turbine, the aerodynamic forces are determined by the instantaneous air velocity distribution along each of the turbine blades. These blades in turn are rotating through the turbulence field which is being convected past the turbine rotor disc. It is thus necessary to characterize the wind turbulence field by a three-dimensional velocity vector which varies randomly with time and with the position in space. A complete statistical description of this turbulent velocity field requires the determination of all possible joint probability distributions between different velocity components at different times and positions in space. Clearly, such a description will not be possible without considerable simplification. The validity of the resulting simplified model will depend upon a comparison of the characteristics predicted by the model and those observed in the atmosphere and more importantly, those observed in actual wind turbine field tests. In this paper we will describe the assumptions and the analytical steps used to arrive at the simplified model. In the accompanying paper the model is used to predict wind turbine response characteristics. It is hoped that these results will be verified in the near future by direct comparison with the results of actual field tests.

2. MODEL ASSUMPTIONS AND APPROXIMATIONS

The first assumption relates to the type of statistical information which is necessary to describe the net aerodynamic forces and moments acting on the turbine rotor. Several authors (2,3) have indicated that the quantities needed for wind turbine design can be obtained from the mean and second-moment statistical characteristics of the various system responses. For stationary processes this information is contained in the mean and power spectral density. In this type of analysis, the mean and power spectral density are characterized by a set of parameters. Rice's theory (4) for computing the frequency of level crossings or peaks is then used with the observed parameter probability densities to obtain the desired response statistics. In this paper, we will strive to determine the power spectral density characteristics of the turbulence. When they are combined with the machine dynamic model, we will assume that the resulting response statistics will be useful for machine design.

The next simplification assumes that the variation in the turbulent velocity observed at a stationary point is due primarily to the convection of the turbulent eddies past the tower. Known as Taylor's frozen field hypothesis (5), this assumption is widely used in reducing fixed-tower, wind turbulence data and correlating these results with data from spatially separated points (6).

The following assumptions which are often used in analyses involving aircraft flying through turbulence are more questionable when applied to turbulence observed in the atmospheric boundary layer. First, when the mean velocity field is subtracted from the total instantaneous velocity field, the resulting turbulent velocity is assumed to be locally homogeneous. Thus, when vertical separations between points are as large as the disc diameter, the correlations are not explicitly height dependent. Second, the field is assumed to be isotropic for all separations for which it is homogeneous. The latter assumption is known not to be precisely correct since the variance of the vertical component is less than the horizontal components (7) and the vertical and downwind components are correlated due to the boundary layer shear of the mean flow (8). However, no model currently exists for predicting the three-dimensional, nonisotropic correlations between velocity components at points separated in space. In the absence of a better model, the isotropic model will be used with the understanding that the results may need adjustment when more complete experimental results are available.

With the previous assumptions (and assuming incompressible flow), Batchelor (9) has shown that the correlation tensor between velocity components at spatially separated points has the form

$$R_{ij}(\vec{\xi}) = \sigma^2[f(\xi)\delta_{ij} + \frac{1}{2}\xi f'(\xi)(\delta_{ij} - \frac{\xi_i\xi_j}{\xi^2})] \quad (2.1)$$

where $R_{ij}(\vec{\xi}) = E[v_i(\vec{x} + \vec{\xi})v_j(\vec{x})]$

$v_i(\vec{x})$ = ith velocity component at position $\vec{x}$

ξ_i = ith component of the separation $\vec{\xi}$

$\xi = \sqrt{\xi_1^2 + \xi_2^2 + \xi_3^2} = |\vec{\xi}|$

δ_{ij} = 1 for i = j and 0 for i ≠ j

$f(\xi)$ = longitudinal correlation function

σ^2 = variance of the turbulent velocity components

Von Karman (10) suggested the form for the longitudinal correlation function

$$f(\xi) = b\left(\frac{\xi}{aL}\right)^{1/3} K_{1/3}\left(\frac{\xi}{aL}\right) \qquad (2.2)$$

where a = 1.339

b = 0.5925

L = integral scale $\triangleq \int_0^\infty f(\xi)d\xi$

$K_{1/3}(\cdot)$ = modified Bessel function of order 1/3

This function results in Kolmogorov's (11) -5/3 power law for the inertial subrange in the longitudinal power spectral density.

At this point, a very useful approximation due to Etkin (12) is introduced. The power of this approximation is that it separates the computation of the aerodynamic responses into two tractable pieces. In the first, the spatial variation of the turbulence is locally approximated by an expansion. The various time varying turbulence components are then multiplied by standard aerodynamic influence coefficients to obtain the required aerodynamic responses. These influence coefficients are the same as those that would be computed in the absence of turbulence. The results of this procedure are extensively used in aircraft response calculations for flight through turbulence (13). The results for the airplane case, however, cannot be applied directly to the wind turbine problem because of major differences in the geometry. The aerodynamic surfaces of an airplane lie in a nearly horizontal plane while the blades of a horizontal axis wind turbine lie in a vertical plane nearly perpendicular to the mean wind. It is necessary then, to rederive the results in a form which is compatible with the wind turbine geometry.

3. DERIVATION OF THE TURBULENCE MODEL

The coordinate definitions used in this paper are shown in Figure 1. In the vacinity of the rotor disc, the turbulent velocity is expressed locally by the approximation

$$\hat{v}_i(r,\theta,t) = V_i(t) + V_{i,x}(t)\, r\sin\theta + V_{i,z}(t)\, r\cos\theta + \text{higher order terms} \qquad (3.1)$$

In this approximation, the spatial randomness of the turbulence is accounted for by the time varying random quantities $V_i(t)$, $V_{i,x}(t)$, $V_{i,z}(t)$ and higher order terms. While this approximation appears to be a Taylor series expansion, it is not. Because of the random nature of the spatial variations, the samples from the statistical ensemble do not have the usual continuity and differentiability properties necessary for a true Taylor expansion. The expansion, however, can be thought of as a functional approximation. Here, the object is to choose the terms in the expansion so as to minimize some measure of the approximation error. When dealing with random functions, a reasonable error measure is its variance. It will be understood that convergence of the approximation series means that the error variance approaches zero as more and more terms are included. Convergence in variance further implies that the series converges in probability (14), i.e.,

$$\lim_{n\to\infty} \Pr\{|e_n| > \varepsilon\} = 0 \quad \text{for all } \varepsilon > 0$$

where e_n is the approximation error including only the nth order terms.

At any given time, the terms V_i, $V_{i,x}$, and $V_{i,z}$ are chosen to minimize the criterion

$$\varepsilon = \frac{1}{A}\int_A \sum_i (\hat{v}_i - v_i)^2\, dA \qquad (3.2)$$

where A = rotor disc area

$\hat{v}_i = V_i + V_{i,x}\, r\sin\theta + V_{i,z}\, r\cos\theta$

$v_i = v_i(r,\theta,t)$

The necessary conditions for the minimization are

$$\frac{\partial\varepsilon}{\partial V_i} = \frac{2}{A}\int_A (\hat{v}_i - v_i)\, dA = 0$$

$$\frac{\partial\varepsilon}{\partial V_{i,x}} = \frac{2}{A}\int_A (\hat{v}_i - v_i)\, r\sin\theta\, dA = 0 \qquad (3.3)$$

$$\frac{\partial\varepsilon}{\partial V_{i,z}} = \frac{2}{A}\int_A (\hat{v}_i - v_i)\, r\cos\theta\, dA = 0$$

which in turn require that

$$V_i(t) = \frac{1}{A}\int_A v_i(r,\theta,t)dA$$

$$V_{i,x}(t) = \frac{1}{I_x}\int_A v_i(r,\theta,t)\, r\sin\theta\, dA \qquad (3.4)$$

$$V_{i,z}(t) = \frac{1}{I_z}\int_A v_i(r,\theta,t)\, r\cos\theta\, dA$$

where $A = \pi R^2$ the disc area

$I_x = I_z = \frac{\pi R^4}{4}$ the area moments about the x and z axes.

Thus, if the statistics of the turbulence field are known, then the statistics of V_i, $V_{i,x}$ and $V_{i,z}$ and any higher order terms can be determined. For example the autocorrelation function for the uniform, through-the-disc component is expressed as

$$R_{V_y}(\tau) \triangleq E\,[V_y(t+\tau)V_y(t)] = \frac{1}{A^2}\int_A\int_A E[v_y(r,\theta,t+\tau)v_y(\rho,\phi,t)]dA_1 dA_2 \qquad (3.5)$$

Using Taylor's hypothesis yields

$$R_{V_y}(\tau) = \frac{1}{A^2}\int_A\int_A R_{22}(\xi_1,\xi_2,\xi_3)dA_1dA_2 \qquad (3.6)$$

where $\xi_1 = r\sin\theta - \rho\sin\phi$

$\xi_2 = V_w\tau$

$\xi_3 = r\cos\theta - \rho\cos\phi$

$dA_1 = rdrd\theta$

$dA_2 = \rho d\rho d\phi$

and V_w = mean wind speed

In the isotropic case,

$$R_{22}(\xi_1,\xi_2,\xi_3) = \sigma^2[f(\xi) + \frac{1}{2}\xi f'(\xi)(\frac{\xi^2 - V_w^2\tau^2}{\xi^2})] \qquad (3.7)$$

where $\xi^2 = \xi_1^2 + \xi_2^2 + \xi_3^2$

$= r^2 + \rho^2 - 2r\rho\cos(\theta-\phi) + V_w^2\tau^2$

Even for the simple exponential correlation function

$$f(\xi) = e^{-\frac{\xi}{L}} \qquad (3.8)$$

it is doubtful that an analytical expression for $R_{V_y}(\tau)$ exists. Hence, numerical integration procedures were employed to perform the required computations. Details of these procedures are found in the Appendix.

At this point, it is convenient to rearrange the gradient terms for the in-plane components. This form is chosen because the resulting terms naturally appear when the velocity is expressed in components which rotate with the turbine blades. These terms can be interpreted as local fluid rotations and strain rates. Thus, the following terms are defined

$$\left.\begin{aligned} \gamma_{xz} &= \frac{1}{2}(V_{z,x} - V_{x,z}) \quad \text{swirl} \\ \bar{\gamma}_{xz} &= \frac{1}{2}(V_{z,x} + V_{x,z}) \\ \varepsilon_{xz} &= \frac{1}{2}(V_{z,z} - V_{x,x}) \end{aligned}\right\} \text{shear strain rates} \qquad (3.9)$$

$$\bar{\varepsilon}_{xz} = \frac{1}{2}(V_{z,z} + V_{x,x}) \quad \text{dilation}$$

Typical fluid streamlines giving rise to positive terms are shown in Figure 2.

Retaining the uniform and gradient terms in the expansion results in the following nine terms which vary randomly with time: V_x, V_y, V_z, $V_{y,x}$, $V_{y,z}$, γ_{xz}, $\bar{\gamma}_{xz}$, ε_{xz}, $\bar{\varepsilon}_{xz}$. The correlation statistics of these terms can be computed using double-area integral expressions similar to Eq. (3.6). Because of the statistical isotropy, it is easily shown that all nine terms are mutually uncorrelated. Thus, all second moment statistics will be determined by the autocorrelation functions or the power spectral densities of the nine terms. Using the scaling parameters in Table 1, nondimensional power spectral density curves can be plotted. These curves will be a one parameter family depending on the ratio of turbine size to turbulence integral scale (R/L). Example curves are shown in Figures 3 and 4.

Table 1. Scaling Parameters for Nondimensional Curves.

Variables	Scaling Parameter
Turbulent velocity, V_i	σ
Velocity gradient, $V_{i,j}$	σ/R
Frequency, ω	V_w/L

Also shown in Figures 3 and 4 are approximate spectra derived from an exponential autocorrelation function. These approximate spectra match the computed spectra at low frequency and have the same total variance. Stationary, random processes with exponential autocorrelation functions can be conveniently represented by stochastic differential equations of the form

$$\dot{x} + ax = bw \qquad (3.10)$$

where x = random process

w = white noise with flat PSD = q

The autocorrelation function and power spectrum are

$$R_x(\tau) = \frac{b^2q}{2a}e^{-a|\tau|} \qquad (3.11)$$

$$S_x(\omega) = \frac{b^2q}{a^2+\omega^2} \qquad (3.12)$$

respectively, from which the parameters a and b can be determined

$$a = \frac{2R_x(0)}{S_x(0)} \qquad (3.13)$$

$$b = \frac{2R_x(0)}{\sqrt{qS_x(0)}} \qquad (3.14)$$

For the wind turbulence it is convenient to choose the white noise, power spectral density

$$q = \frac{\sigma^2L}{V_w^3} \qquad (3.15)$$

Nondimensional parameters can thus be defined

$$a_* \triangleq \frac{La}{V_w} = \frac{2LR_x(0)}{V_wS_x(0)} \qquad (3.16)$$

$$b_* \triangleq \begin{cases} \dfrac{Lb}{V_w^2} = \dfrac{2\left(\dfrac{R_x(0)}{\sigma^2}\right)}{\sqrt{\dfrac{V_w S_x(0)}{L\sigma^2}}} & \text{uniform terms} \\ \dfrac{RLb}{V_w^2} = \dfrac{2\left(\dfrac{R^2 R_x(0)}{\sigma^2}\right)}{\sqrt{\dfrac{V_w R^2 S_x(0)}{L\sigma^2}}} & \text{gradient terms} \end{cases} \tag{3.17}$$

which will depend only on the ratio R/L. As an example of the computational procedure, consider the turbulence component V_y. In this case,

$$\frac{R_x(0)}{\sigma^2} = \frac{1}{A^2}\int_A\int_A g\left(\frac{\xi}{L}, 0\right) dA_1 dA_2 \tag{3.18}$$

and

$$\frac{V_w S_x(0)}{L\sigma^2} = \frac{2}{A^2}\int_0^\infty\int_A\int_A g\left(\frac{\xi}{L}, \frac{V_w\tau}{L}\right) dA_1 dA_2 \left(\frac{V_w}{L}\right) d\tau \tag{3.19}$$

where $g\left(\frac{\xi}{L}, \frac{V_w\tau}{L}\right) = f(\xi) + \frac{1}{2}\xi f'(\xi)\left(\frac{\xi^2 - V_w^2\tau^2}{\xi^2}\right)$

$$\xi = \sqrt{r^2 + \rho^2 - 2r\rho\cos(\theta-\phi) + V_w^2\tau^2}$$

$$dA_1 = r\,dr\,d\theta$$

$$dA_2 = \rho\,d\rho\,d\phi$$

and $f(\cdot)$ is the isotropic correlation function.

The results of numerical computations for these integrals are shown in Figures 5-8 for all of the turbulence components.

In summary, each of the turbulence terms are modeled by stochastic differential equations of the form

$$\dot{x} = ax + bw \tag{3.20}$$

where x = instantaneous value of one of the terms V_x, ..., $V_{y,x}$, ..., γ_{xz}, etc.

w = nondimensional white noise with power spectral density $q = \sigma^2 L/V_w^3$

$$a = \frac{V_w}{L} a_* \tag{3.21}$$

$$b = \begin{cases} \dfrac{V_w^2}{L} b_* & \text{for uniform terms} \\ \dfrac{V_w^2}{LR} b_* & \text{for gradient terms} \end{cases} \tag{3.22}$$

The nondimensional terms a_* and b_* are found from Figures 5-8 as appropriate and depend on the ratio of turbine size to turbulence scale (R/L). Power spectral densities can be obtained if desired from the equation

$$S_x(\omega) = \frac{b^2 q}{a^2+\omega^2} \tag{3.23}$$

4. MODEL ERROR DISCUSSION

Three levels of approximation are introduced in this paper. In the first, the turbulence is modeled as locally homogeneous and isotropic with correlations given by the Von Karman model. This assumption probably introduces the largest amount of error in the model. Several authors (15,16) indicate that the horizontal velocity components have a variance which is approximately three times the variance of the vertical component. If we assume that the turbulent velocity predicted by the isotropic model has a vertical component which is $\sqrt{3}$ times too large, but is otherwise statistically correct, then the velocity error magnitude introduced has a variance

$$\begin{aligned} \varepsilon &\triangleq E\left[\sum_{i=1}^{3} (\hat{v}_i - v_i)^2\right] \\ &= E\left[(\sqrt{3}\, v_3 - v_3)^2\right] \\ &= (\sqrt{3} - 1)^2\left(\tfrac{1}{3}\sigma^2\right) \\ &= 0.18\,\sigma^2 \end{aligned} \tag{4.1}$$

where σ^2 = variance of horizontal components.

The second level of approximation occurs in truncating the higher order terms in the spatial expansion. Thus, at any point on the rotor disc, the turbulent velocity is approximated by

$$\hat{v}_i(r,\theta,t) = V_i(t) + V_{i,x}(t) r\sin\theta + V_{i,z}(t) r\cos\theta \tag{4.2}$$

Since the velocity component through the rotor, V_y, produces the greatest aerodynamic force, consider the error variance produced by the approximation of this component

$$\varepsilon_1(r,\theta) = \frac{1}{\sigma^2} E[(\hat{v}_y(r,\theta,t) - v_y(r,\theta,t))^2] \tag{4.3}$$

Averaging over the rotor disc gives

$$\bar{\varepsilon}_1 = \frac{1}{A}\int_A \varepsilon_1(r,\theta)\, dA \tag{4.4}$$

Using the relations for terms $V_y(t)$, $V_{y,x}(t)$ and $V_{y,z}(t)$ given by Equations 3.4 yields the useful relation

$$\int_A (\hat{v}_y - v_y)\hat{v}_y\, dA = 0 \tag{4.5}$$

and hence

$$\bar{\varepsilon}_1 = \frac{1}{A\sigma^2}\int_A E[\hat{v}_y^2]dA - \frac{1}{A\sigma^2}\int_A E[\hat{v}_y v_y]dA$$

$$= 1 - \frac{1}{\sigma^2}E[V_y^2] - \frac{I_x}{A\sigma^2}E[V_{y,x}^2] - \frac{I_3}{A\sigma^2}E[V_{y,z}^2] \quad (4.6)$$

which finally gives

$$\bar{\varepsilon}_1 = 1 - \frac{R_{V_y}(0)}{\sigma^2} - \frac{1}{4}\frac{R^2 R_{V_{y,x}}(0)}{\sigma^2} - \frac{1}{4}\frac{R^2 R_{V_{y,z}}(0)}{\sigma^2} \quad (4.7)$$

This quantity can be interpreted as a measure of the total variance of the part of the turbulent velocity that is not included in the model. Thus, the averaged error, $\bar{\varepsilon}_1$ is zero if the approximation is "perfect",

and $\bar{\varepsilon}_1 = 1$ if the trivial approximation $\hat{v}_y = 0$ is used.

In a similar fashion the quantity $\bar{\varepsilon}_0$ can be defined when only the uniform terms are retained and $\bar{\varepsilon}_2$ when uniform, gradient, and quadratic terms are retained. Table 2 shows the effect of increasing rotor size relative to the turbulence scale.

Table 2 - Relative Approximation Error Variance

$\frac{R}{L}$	$\bar{\varepsilon}_0$	$\bar{\varepsilon}_1$	$\bar{\varepsilon}_2$
.01	.044	.026	.023
.054(Mod M)	.135	.081	.070
.1	.201	.121	.105
.3(Mod G)	.397	.250	.218
.5	.527	.348	.304
1.0	.724	.527	.465
2.0	.889	.737	.663

Observing the results given in this table, a significant improvement is obtained when the gradient terms are included along with the uniform term. However, only a small improvement is obtained when the quadratic terms are also included. This leads to the conclusion that the unmodeled portion of the turbulence is highly disorganized and probably has a negligible effect on the forces and moments felt at the hub.

To investigate this effect further, the following aerodynamic model was assumed for a light, rigid blade cutting through the turbulent velocity field

$$f(t) = \frac{3C}{R^3}\int_0^R r\sqrt{R^2-r^2}\; v_y(r,\Omega t,t)dr \quad (4.8)$$

where f = the net blade force (torque or thrust deviation from nominal)
C = the aerodynamic influence coefficient
Ω = rotation rate of the rotor
and $v_y(r,\theta,t)$ = instantaneous turbulent velocity.

Note, for a steady, uniform velocity, the force is constant and given by

$$f = C\, v_y$$

Now, let the approximate force be the result of the uniform and gradient terms in the model. Thus,

$$\hat{f}(t) = \frac{3C}{R^3}\int_0^R r\sqrt{R^2-r^2}\;\hat{v}_y(r,\Omega t,t)\,dr \quad (4.9)$$

where $\hat{v}_y = V_y(t) + V_{y,x}(t)r\sin\Omega t + V_{y,z}(t)r\cos\Omega t$

Integrating along the blade yields

$$\hat{f}(t) = C[V_y(t) + \frac{3\pi}{16}R(V_{y,x}(t)\sin\Omega t + V_{y,z}(t)\cos\Omega t)] \quad (4.10)$$

The relative error variance is given by

$$\varepsilon_1 = \frac{E[(\hat{f}-f)^2]}{E[f^2]} = \frac{E[\hat{f}^2] - 2E[\hat{f}f] + E[f^2]}{E[f^2]} \quad (4.11)$$

Substituting Equations 4.10 and 4.8 into these variance terms gives

$$E[\hat{f}^2] = C^2[R_{V_y}(0) + (\frac{3\pi R}{16})^2(R_{V_{y,x}}(0)\sin^2\Omega t + R_{V_{y,z}}(0)\cos^2\Omega t)] \quad (4.12)$$

$$E[f^2] = \frac{9C^2}{R^6}\int_0^R\int_0^R r\rho\sqrt{(R^2-r^2)(R^2-\rho^2)}\;R_{22}(\xi_1,0,\xi_3)dr d\rho \quad (4.13)$$

where $\xi_1 = (r-\rho)\sin\Omega t$

$\xi_3 = (r-\rho)\cos\Omega t$

$R_{22}(\cdot,\cdot,\cdot)$ = turbulent velocity correlation function

$$E[\hat{f}f] = C^2(I_0 + I_1) \quad (4.14)$$

where

$$I_0 = \frac{3}{\pi R^5}\int_0^R\int_A r\sqrt{R^2-r^2}\;R_{22}(\xi_1,0,\xi_3)dA dr$$

$$I_1 = \frac{9}{4R^6}\int_0^R\int_A r\sqrt{R^2-r^2}\;\rho\cos(\phi-\Omega t)R_{22}(\xi_1,0,\xi_3)dA dr$$

$$\xi_1 = r\sin\Omega t - \rho\sin\phi$$

$$\xi_3 = r\cos\Omega t - \rho\cos\phi$$

$$dA = \rho d\rho d\phi$$

The normalized error variance, ε_0, defined by neglecting the gradient terms in the approximate velocity, is determined in a similar way. Table 3 shows the results of these computations

Table 3 - Relative Blade Force Error Variance

$\frac{R}{L}$	ε_0	ε_1
.01	.024	.009
.054(Mod M)	.076	.030
.1	.116	.046
.3(Mod G)	.248	.104
.5	.350	.157
1.0	.536	.278
2.0	.753	.488

Comparing the results of Table 3 and Table 2, it is seen that only half the unmodeled velocity variance is observed as unmodeled force variance. This result is due to the averaging effect of the integration along the blade. If the blade were more realistically modeled with inertia it is expected that little of the remaining unmodeled variance would be transmitted to the hub.

The third level of approximation involves the use of the stochastic differential equation (Equation 3.20) to model the uniform and gradient turbulence components. The accuracy of this approximation depends on how close the spectral form

$$S_x(\omega) = \frac{b^2 q}{a^2 + \omega^2}$$

is to the spectra computed by integration. Figures 3 and 4 show two examples of such a comparison. The parameters a and b are chosen so that the total variance and the low frequency spectrum for the model are correct.

Considering the results of these error calculations, it is reasonable to expect that the turbulence inputs described statistically by the model will approximate the effect of the true turbulence on the wind turbine. Realistic evaluation of the modeling error, however, can only be accomplished by comparison with experimental data. It is hoped that such a comparison can be made in the near future.

5. AERODYNAMIC FORCE ON ROTATING WIND TURBINE BLADE

As an illustration of how the turbulence interacts with a rotating turbine blade, consider the previous example of a rigid blade rotating in the turbulent velocity field. Using the approximate turbulence model, the blade force is given by

$$f(t)=C[V_y(t)+\tfrac{3\pi}{16} R(V_{y,x}(t)\sin\Omega t+V_{y,z}(t)\cos\Omega t)] \quad (5.1)$$

Defining the three components of the dynamic state vector

$$\left.\begin{aligned} x_1(t) &= V_y(t) \\ x_2(t) &= \cos\Omega t\, V_{y,z}(t) + \sin\Omega t\, V_{y,x}(t) \\ x_3(t) &= -\sin\Omega t\, V_{y,z}(t) + \cos\Omega t\, V_{y,x}(t) \end{aligned}\right\} \quad (5.2)$$

yields the stochastic differential equations

$$\dot{x}_1 = -a_1 x_1 + b_1 w_1 \quad (5.3)$$

$$\dot{x}_2 = -a_2 x_2 + \Omega x_3 + b_2 w_2 \quad (5.4)$$

and $$\dot{x}_3 = -\Omega x_2 - a_2 x_3 + b_2 w_3 \quad (5.5)$$

Since the original white noise inputs are uncorrelated with identical power spectral densities, it can be shown that w_2 and w_3 are also uncorrelated white noise processes with the same power spectral density. This yields the following matrix form for the stochastic differential equations

$$\begin{aligned} \{\dot{x}\} &= [A]\{x\} + [B]\{w\} \\ \{f\} &= [C]\{x\} \end{aligned} \quad (5.6)$$

where the matrices are given by

$$\left.\begin{aligned} [A] &= \begin{bmatrix} -a_1 & 0 & 0 \\ 0 & -a_2 & \Omega \\ 0 & -\Omega & -a_2 \end{bmatrix} \\ [B] &= \begin{bmatrix} b_1 & 0 & 0 \\ 0 & b_2 & 0 \\ 0 & 0 & b_2 \end{bmatrix} \\ [C] &= [C,\ C\,\tfrac{3\pi}{16} R,\ 0] \end{aligned}\right\} \quad (5.7)$$

Using these equations the output power spectral density is given by the well known expression (17)

$$S_f(\omega) = [H(i\omega)][Q][H^T(-i\omega)] \quad (5.8)$$

where the row matrix of transfer functions is given by

$$[H(i\omega)] = [C][i\omega I - A]^{-1}[B] \quad (5.9)$$

Since the elements of the noise vector are uncorrelated and have identical power spectral densities

$$[Q] = \begin{bmatrix} q & 0 & 0 \\ 0 & q & 0 \\ 0 & 0 & q \end{bmatrix} \quad (5.10)$$

which gives

$$\begin{aligned} S_f(\omega) &= q[H(i\omega)][H^T(-i\omega)] \\ &= q \sum_k |H_{jk}(i\omega)|^2 \end{aligned} \quad (5.11)$$

For the case at hand,

$$[H(i\omega)] = \left[\frac{Cb_1}{a_1+i\omega},\ \frac{C\,\frac{3\pi}{16} R\, b_2(a_2+i\omega)}{(a_2+i\omega)^2+\Omega^2},\ \frac{C\,\frac{3\pi}{16} R\, b_2\Omega}{(a_2+i\omega)^2+\Omega^2}\right] \quad (5.12)$$

and

$$S_f(\omega) = \frac{(Cb_1)^2 q}{a_1^2+\omega^2} + \frac{(C\,\frac{3\pi}{16} R\, b_2)^2(a_2^2+\Omega^2+\omega^2)q}{(a_2^2+\Omega^2+\omega^2)^2-(2\Omega\omega)^2} \quad (5.13)$$

Using the non-dimensional terms defined in Equations 3.16 and 3.17 yields the result

$$\frac{V_w S_f(\omega)}{C^2\sigma^2 L} = \frac{b_{*1}^2}{a_{*1}^2+\omega_*^2} + \frac{(\frac{3\pi}{16} b_{*2})^2(a_{*2}^2 + \Omega_*^2 + \omega_*^2)}{(a_{*2}^2 + \Omega_*^2 + \omega_*^2)^2-(2\,\Omega_*\omega_*)^2} \tag{3.14}$$

where the non-dimensional frequencies are defined by

$$\omega_* = \frac{L\omega}{V_w} \quad \text{and} \quad \Omega_* = \frac{L\Omega}{V_w} \tag{3.15}$$

The non-dimensional, power spectral density from Equation 3.14 is plotted in Figure 9. The parameters for these blades were selected to correspond to two typical wind turbines of vastly different size. Table 4 provides the key parameters for these two turbines.

Table 4 - Parameters for Typical Wind Turbines

	Mod M	Mod G
Radius, R (ft)	16.67	150
Rated Power	8 kW	2.5 MW
Windspeed, V_w (m.p.h.)	16.63	20
Rotation Rate, Ω (rpm)	73.35	17.5
Turbulence Scale, L (ft)	300	500

It is clear from Figure 9 that the effect of blade rotation is to concentrate the variance due to the turbulence gradient components at a frequency equal the rotation rate. This effect can be understood by considering the blade to be slicing through a slowly varying velocity gradient. As the blade encounters the higher velocity on one side of the rotor disc the force is increased. As it moves through 180° the force reaches a minimum giving a fluctuating force at the rotor frequency. The importance of this effect can be seen by comparing the relative contributions of the uniform and gradient components to the total variance of the blade force. Table 5 shows these results.

Table 5 - Relative Contributions to Blade Force Variance

	Uniform Term	Gradient Terms
Mod M (8 kW)	96%	4%
Mod G (2.5 MW)	85%	15%

Clearly for the larger blade, 15% of the variance at the relatively high rotor frequency could cause more fatigue damage than the 85% for the uniform component at the lower frequencies.

6. CONCLUSIONS

In this paper, we have formulated a theoretical model for the wind turbulence as it affects horizontal axis wind turbines. The model includes the effect of variations in the turbulent velocity across the rotor disc. An indication of the approximation error in the model has also been given. It is expected that the model will be useful for determining how important the different turbulence effects are for given machine responses. This type of study has been made in the accompanying paper (1). While we believe that the model will give qualitatively correct results, it is important that experimental verification and any necessary model adjustments be made before it is used for design purposes.

ACKNOWLEDGEMENT

This research was supported by the Department of Energy through Battelle, Pacific Northwest Laboratory, under contract DE-AT06-79ET23144. The authors wish particularly to thank Dr. J.R. Connell, the technical monitor, for his enthusiastic support and the PNL staff for their many valuable suggestions.

APPENDIX

Numerical Procedures Utilized in Model Development

A.1 Area Integration Over Rotor Disc

Two Gaussian quadrature formulas (18) were utilized to perform area integrations over the rotor disc. The distribution of points is shown in Figure 10 and given in Tables 6 and 7.

Table 6 - Sixteen Point Formula

r_i	C_i
.21132487	.19634954
.78867513	.19634954

Table 7 - Sixty-four Point Formula

r_i	C_i
.26349923	.03415057
.57446451	.06402420
.81852949	.06402420
.96465961	.03415057

The quadrature formulas have the following form:

$$\int_A f(r,\theta)dA = \sum_{i=1}^{n} \sum_{j=1}^{4n} C_i f(r_i,\theta_j)$$

$$\theta_j = \frac{\pi j}{2n}$$

A six-point formula was also developed to reduce the computational load. In this case, the radius was adjusted until the best match between computations using the sixty-four-point formula and the six-point formula was achieved and resulted in r = 0.69. For all computations, comparison was made between two formulas to verify accuracy to within five percent.

A.2 Integration Along Radius

An eight-point Gaussian quadrature formula (19) was utilized for radial integrations where required without angle dependence.

$$\int_0^1 f(r)dr = \sum_{i=1}^{n} C_i f(r_i)$$

The weights and absissas are given in Table 8.

Table 8 - Radial Quadrature Formula

r_i	C_i
.0198550717	.0506142681
.1016667612	.1111905172
.2372337950	.1568533229
.4082826787	.1813418916
.5917173212	.1813418916
.7627662049	.1568533229
.8983332387	.1111905172
.9801449282	.0506142681

A.3 Fourier Transforms

For calculation of power spectral densities the Fourier transform defined by

$$S(\omega) = \int_{-\infty}^{+\infty} e^{-i\omega\tau} R(\tau)d\tau$$

was numerically computed from the autocorrelation function using the finite approximation

$$S(\omega_k) = \frac{T}{2n}\left(2\mathrm{Re}\left[\sum_{j=0}^{n} R(\tau_j)e^{-i\omega_k\tau_j}\right]-R(o)\right)$$

where $\omega_k = \left(\frac{4\pi n}{T(n+1)}\right)k$

$$\tau_j = \left(\frac{T}{2n}\right)j$$

The fast Fourier transform techniques of the IMSL (20) library routine FFTRC were utilized. Several different time intervals were chosen to give overlapping spectra over the different frequency decades.

A.4 Semi-Infinite Time Interval

To calculate the zero frequency power spectra, a Gaussian quadrature formula (21) was utilized.

$$\int_0^{\infty} e^{-x} f(x)dx = \sum_{i=1}^{n} C_i f(x_i)$$

The absissas and weights for the sixteen points are given in Table 9.

Table 9 - Semi-Infinite Interval Quadrature Formula

x_i	C_i
.087649	.206152
.46270	.331058
1.14106	.265796
2.12928	.136297
3.43709	.473289 E-01
5.07802	.113000 E-01
7.07034	.184910 E-02
9.43831	.204272 E-03
12.21422	.148446 E-04
15.44153	.682832 E-06
19.18016	.188100 E-07
23.51591	.286235 E-09
28.57873	.212708 E-11
34.58340	.629797 E-14
41.94045	.505047 E-17
51.70116	.416146 E-21

A.5 Von Karman Correlation Function

Central to all of the previous numerical integration procedures is the need to compute the integrand. In this case the integrand will involve the evaluation of

$$f(\mu) = b\left(\frac{\mu}{a}\right)^{1/3} K_{1/3}\left(\frac{\mu}{a}\right)$$

and

$$g(\mu) = \frac{1}{2}\mu f'(\mu)$$

where $K_{1/3}(\cdot)$ = Modified Bessel function order of 1/3

These functions are evaluated by the subroutine VK developed by Holley and Bryson (22). The method utilizes spline interpolation and asymptotic expansion giving a result accurate to six significant figures over a wide range of arguments.

REFERENCES

1. Thresher, R.W., Holley, W.E. and Jafarey, N., "Wind Response Characteristics of Horizontal Axis Wind Turbines," Proc. Second DOE/NASA Wind Turbine Dynamics Workshop, Cleveland, Ohio, Feb. 24-26, 1981.

2. Frost, W., Long, B.H. and Turner, R.E., Engineering Handbook on the Atmospheric Environmental Guidelines for Use in Wind Turbine Generator Development, NASA Technical Paper 1359, Dec. 1978, p. 4.10-4.42.

3. Powell, D.C. and Connell, J.R., Definition of Gust Model Concepts and Review of Gust Models, Battelle, Pacific Northwest Laboratory, PNL-3138, June 1980, Section 4.

4. Rice, S.O., "Mathematical Analysis of Random Noise," Bell System Technical Journal, V. 24, n. 1 (1945), pp. 46-156.

5. Taylor, G.I., "Eddy Motion in the Atmosphere," Phil. Trans. of the Royal Soc., London, V. A215 (1915), pp. 14-22.

6. Kaimal, J.C., "Turbulence Spectra, Length Scales and Structure Parameters in the Stable Surface Layer," Boundary Layer Meteorology, V. 4 (1973), p. 300.

7. Panofsky, H.A., et. al., "The Characteristics of Turbulent Velocity Components in the Surface Layer Under Convective Conditions," Boundary Layer Meteorology, V. 11 (1977), pp. 355-361.

8. Busch, N.E., "The Surface Boundary Layer," Boundary Layer Meteorology, V. 4 (1973), pp. 213-240.

9. Batchelor, G.K., The Theory of Homogeneous Turbulence, Cambridge, 1953, pp. 169-187.

10. Von Karman, T., "Sur la Theorie Statistique de la Turbulence," Comptes Rendus des Seanies de l'Academie de Sciences, V. 226 (1948), pp. 2108-2111.

11. Kolmogonov, A.N., "The Local Structure of Turbulence in Incompressible Viscous Fluid for Very Large Reynolds Numbers," Doklady Acad. of Science, USSR, V. 30 (1941), p. 301.

12. Etkin, B., Theory of Flight of Airplanes in Isotropic Turbulence, AGARD Report 372, 1961.

13. Chalk, C.R., et. al., Background Information and User Guide for MIL-F-8785B, AFFDL-TR-69-72, Aug. 1969.

14. Melsa, J.L. and Sage, A.P., Estimation Theory with Applications to Communications and Control, McGraw-Hill, 1971, p. 35.

15. Panofsky, 1977, loc. cit.

16. Counihan, J., "Adiabatic Atmospheric Boundary Layers: A Review and Analysis of Data from the Period 1880-1972," Atmospheric Environment, V. 9 (1975), pp. 871-905.

17. Goodwin, G.C. and Payne, R.L., Dynamic System Identification, Acad. Press., 1977, pp. 229-232.

18. Pierce, W.H., "Numerical Integration Over the Planar Annulus," J. Soc. Indust. Appl. Math., V. 5 (1957), pp. 66-73.

19. Stroud, A.H. and Secrest, D., "Gaussian Quadrature Formulas," Prentice-Hall (1966), p. 256.

20. IMSL, Inc., IMSL Library Ref. Manual, 7500 Bellaire Blvd., Houston, TX 77036, p. FFTRC-1.

21. Stroud (1966) loc. cit.

22. Holley, W.E. and Bryson, A.E., Wind Modeling and Lateral Aircraft Control for Automatic Landing, Dept. of Aeronautics and Astronautics, Stanford University, SUDAAR #489 (1975), pp. 78-80.

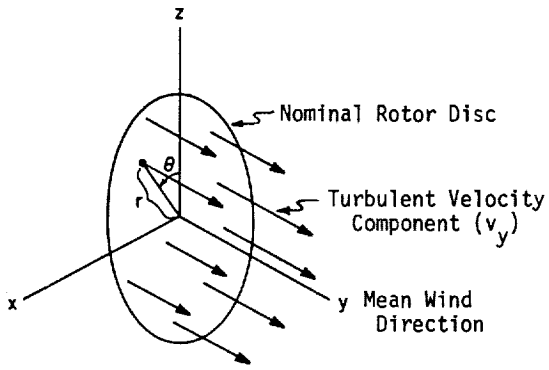

Figure 1: Rotor Disc Coordinates

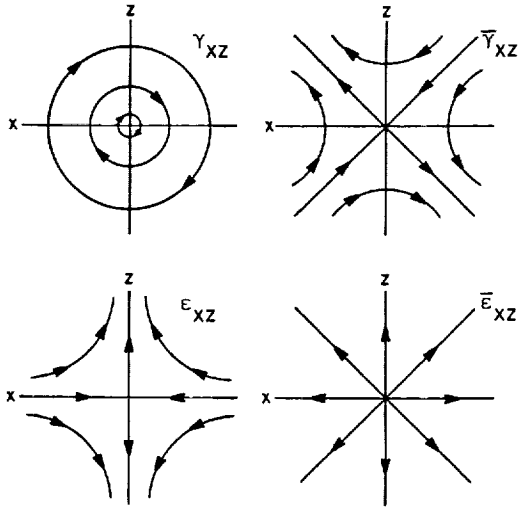

Figure 2: In-Plane Velocity Gradient Terms

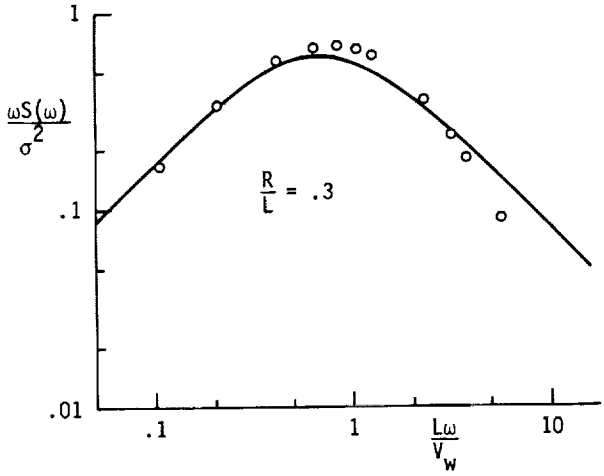

Figure 3: Dimensionless Spectrum for Uniform V_y Turbulence Component

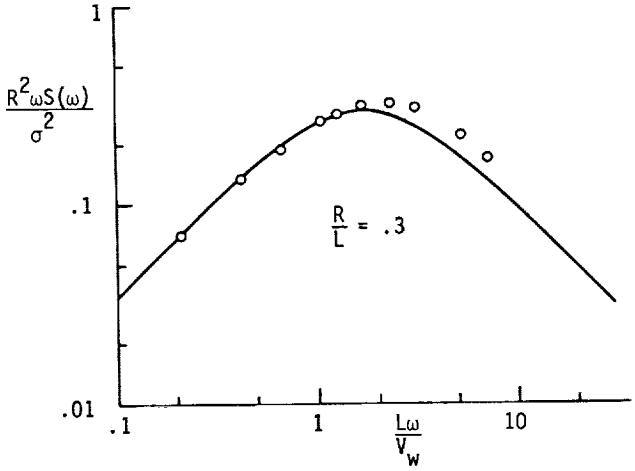

Figure 4: Dimensionless Spectrum for Gradient $V_{y,x}$ Turbulence Component

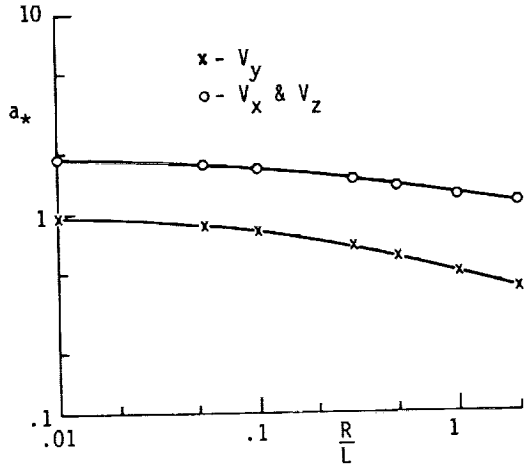

Figure 5: Dimensionless Parameter a_* for Uniform Turbulence Terms

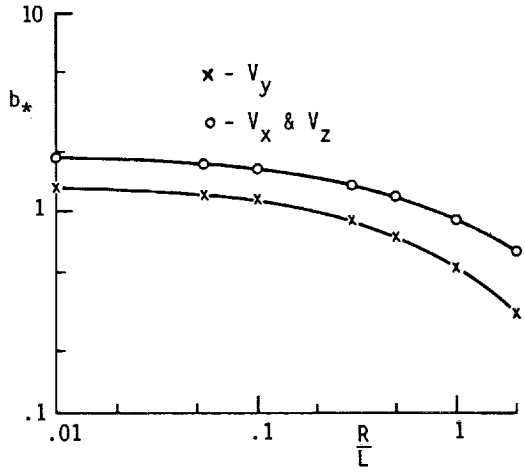

Figure 6: Dimensionless Parameter b_* for Uniform Turbulence Terms

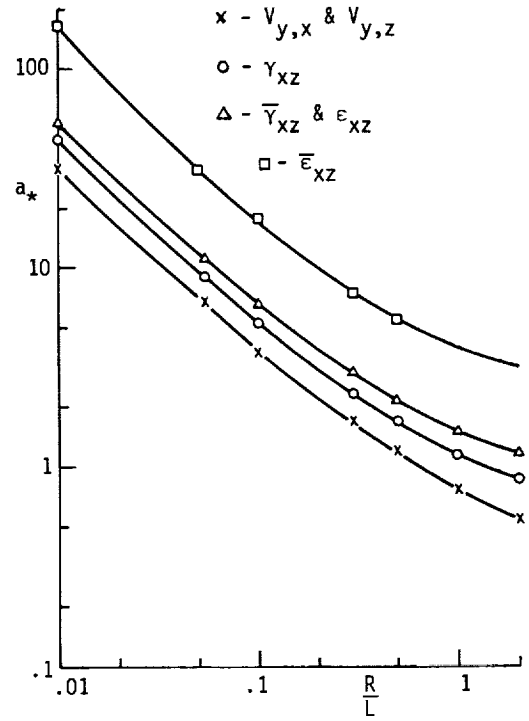

Figure 7: Dimensionless Parameter a_* for Gradient Turbulence Terms

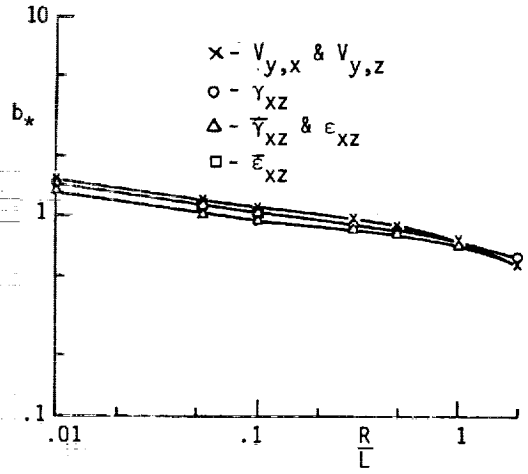

Figure 8: Dimensionless Parameter b_* for Gradient Turbulence Terms

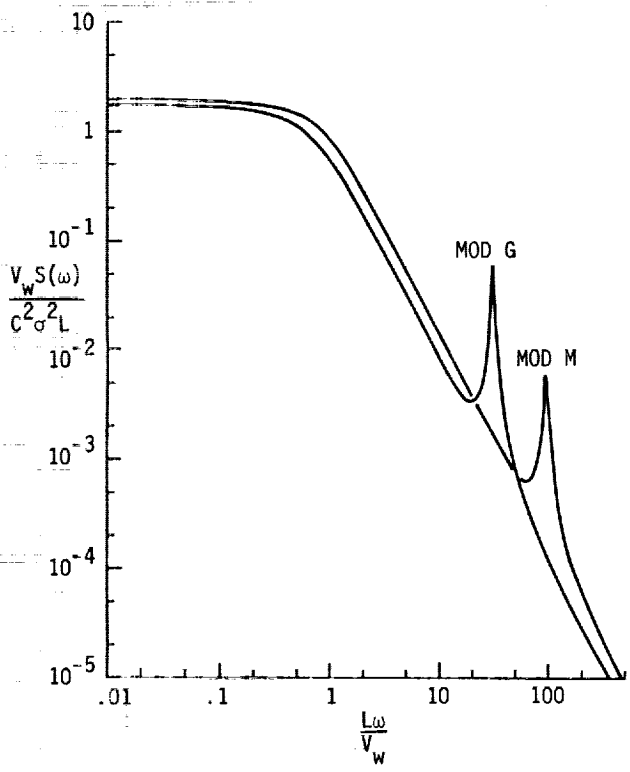

Figure 9: Dimensionless Spectrum for Rotating Blade Force

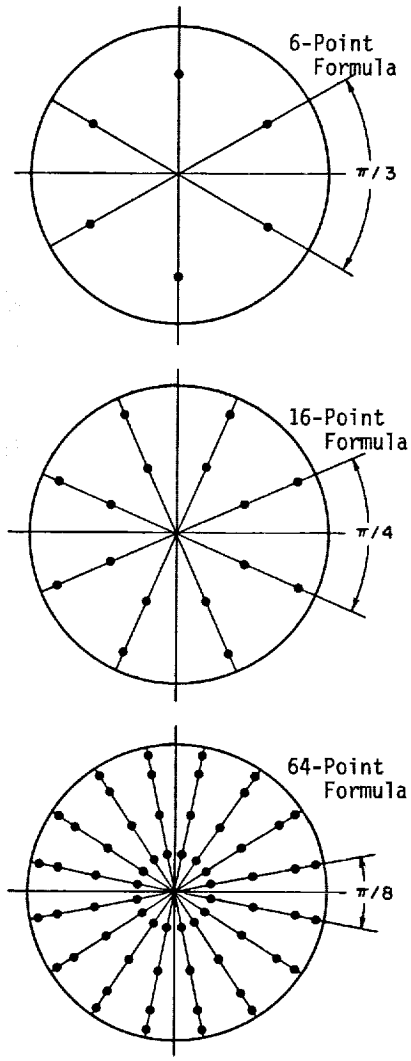

Figure 10: Unit Circle Point Distribution for Disc Area Integration

QUESTIONS AND ANSWERS

W.E. Holley

From: L.P. Rowley

Q: How would you propose verifying your model?

A: *We intend to compare the statistical results predicted by the model with results gained from a planar anemometer array. This comparison can be accomplished using results developed in system identification theory. We also would like to compare model predictions with wind turbine field data.*

From: T.E. Base

Q: Does your turbulence model satisfy the conservation equation, i.e., continuity?

A: *Yes, the Von Karman correlation function satisfies the constraint imposed by the continuity equation. To the degree that the model approximates the Von Karman correlation function, it also satisfies continuity.*

From: L. Mirandy

Q: Is the only spatial effect in your model due to rsin θ, rcos θ terms (gradients $V_{i,x}$, $V_{i,z}$ depend only on time) or do you have a spatial correlation like Dr. Sundar?

A: *The spatial variation effect includes only rsinθ and rcosθ effects. Other more disorganized spatial variations are ignored. These higher order terms are the source of the error discussed in the paper.*